In Situ Spectroelectrochemical Studies of the Decomposition of Hydroquinones on Platinum Electrodes in Dichloromethane Solutions

Ali Babaei and A. James McQuillan*

Department of Chemistry, University of Otago, P.O. Box 56, Dunedin, New Zealand

Received: January 8, 1997; In Final Form: July 2, 1997[⊗]

The decomposition of hydroquinone and of 2,5-di-*tert*-butylhydroquinone in dichloromethane solutions has been studied by *in situ* UV absorption and by *in situ* infrared reflection−absorption spectroelectrochemical methods. The UV absorption spectra showed that benzoquinone and 2,5-di-*tert*-butylbenzoquinone are respective products of these decompositions. The infrared spectra confirmed that the quinones were the principal reaction products but also indicated that some water was formed during the decomposition processes. The decomposition rates were found to be dependent on electrode potential with a minimum rate corresponding to a maximum coverage for adsorbed hydrogen, a product of the decomposition. A new infrared absorption at 1713 cm^{-1} has been detected at positive potentials in the hydoquinone system and has been ascribed to endwise adsorbed benzoquinone.

Introduction

The chemisorption of hydroquinones on platinum electrodes in acidic aqueous solutions has been frequently studied.[1−7] Hubbard et al.[8−11] have shown, from thin layer cell coulometric studies, that hydroquinones adsorb with different surface orientations, depending on the solution concentration and on the steric influences of ring substituents. At low concentrations, e.g., below 10^{-4} M for hydroquinone (BQH_2), adsorption is with the aromatic ring parallel to the surface in an η^6 orientation. At higher concentrations, e.g., above 10^{-3} M for BQH_2, the adsorption is with the aromatic ring edgewise to the surface in an η^2 orientation. There has been only one infrared spectroscopic study directed to establishing adsorbate orientation in the hydroquinone/benzoquinone system.[12] This *ex situ* work from the C−H stretching region showed a similarity between the spectra of adsorbed hydroquinone and of adsorbed benzoquinone (BQ), suggesting that they both adsorb as η^2-bridged quinols. However, the strong absorptions of water in the O−H stretching spectral region prevented any definite conclusions about the orientation of adsorbed hydroquinone.

Hydroquinones adsorbed from aqueous solutions have been shown to decompose to their corresponding quinones and to other products. BQH_2 adsorbed at ∼0.4 V(SHE) with the η^6 orientation decomposes to adsorbed η^6-BQ and hydrogen.[11] BQH_2 adsorption at ∼0.4 V(SHE) with the η^2 orientation is claimed to give an adsorbed η^2-bridged quinol species and hydrogen as a result of hydrogen atom abstraction from the 2,3-C−H bonds.[11] It has been suggested that at more positive potentials the η^6-adsorbed BQ is oxidized to CO_2 while the adsorbed η^2-bridged quinol species is oxidized to maleic acid.[13] It was concluded that the packing density, orientation, and reactivity of quinols at a given concentration were independent of potential of adsorption in the range $0.2\ V < E < 0.7\ V$ (SHE).[4]

Only a few studies have been carried out on the adsorption of hydroquinones to platinum electrodes in nonaqueous solutions.[14−16] It was concluded that benzene, acetonitrile, dimethyl sulfoxide, sulfolane, and dimethylacetamide in dilute aqueous mixtures strongly chemisorb onto platinum and interfere with the adsorption of typical aromatic compounds.[7]

The more strongly adsorbing solvents are claimed to virtually eliminate the flat orientation of aromatics. The coordinating ability of acetonitrile leads to its significant adsorption to platinum. However, dichloromethane has little tendency to adsorb to platinum.[17]

This paper reports the results of *in situ* spectroelectrochemical studies of the decomposition of BQH_2 and of 2,5-di-*tert*-butylhydroquinone ($TBQH_2$) on a platinum electrode in dichloromethane solution. UV absorption spectroelectrochemistry showed that the corresponding quinones are products of the decompositions and that their production rates are potential dependent. The infrared spectroelectrochemistry showed that the corresponding quinones are the principal products of the decompositions but that water is also formed. The infrared spectra revealed that some BQ is adsorbed endwise on platinum in dichloromethane solution.

Experimental Section

Hydroquinone (Fisons, AR) and 2,5-di-*tert*-butyl hydroquinone (Kodak, PG) were recrystallized from hot ethanol, respectively, and dried at 90 °C under vacuum. 1,4-Benzoquinone (BDH, technical) was purified by Soxhlet extraction with hexane, crystallized, and sublimed[18] under reduced pressure at 35 °C. 2,5-Di-*tert*-butylbenzoquinone was prepared by controlled-potential electrolysis of the corresponding quinol. Tetrabutylammonium perchlorate (TBAP) (Fluka, AR) was recrystallized twice from ethyl acetate−pentane and dried for 2 days at 100 °C under reduced pressure.[19] Dichloromethane (BDH, AR) was distilled twice and passed through a column of activated neutral alumina[20] immediately before use. All solutions were purged with oxygen-free nitrogen before measurements.

Cyclic voltammetry was carried out at 20 °C with a PC-controlled EG&G PAR 273A potentiostat. A conventional electrochemical cell was used with a 0.7 mm diameter platinum disc electrode, platinum wire auxiliary electrode, and aqueous KCl saturated calomel reference electrode (SCE) in a separate tube with a Luggin capillary. The platinum electrode was cleaned by successive polishing with alumina powder (BDH) of 0.3, 0.075, and 0.015 μm grades on a Buehler microcloth and final sonication in distilled water.

UV spectroelectrochemistry was carried out with a PC-controlled Perkin-Elmer Lamda 9 spectrometer at a resolution

* To whom correspondence should be addressed.

[⊗] Abstract published in *Advance ACS Abstracts,* August 15, 1997.

S1089-5647(97)00131-4 CCC: $14.00

of 2 nm and with an optically transparent thin layer electrode (OTTLE) cell at 25 °C. The OTTLE cell was constructed from quartz, and the working electrode was a platinum gauze situated in a 0.53 mm optical path length section of the cell. The cell design, with platinum auxiliary electrode and silver wire pseudo-reference electrode, was similar to that previously published.[21] The potential of the silver pseudo-reference electrode, in dichloromethane solution containing 0.2 M TBAP, was ±0.02 V (SCE). Thus, all reported potentials are with respect to the the SCE.

The platinum gauze electrode was cleaned by brief immersion in concentrated nitric acid, washed with distilled water, and electrolyzed in 1 M aqueous H_2SO_4 solution with a platinum auxiliary electrode. The electrolysis treatment was initially a 10 V s^{-1} cycle between −5.0 and 5.0 V for 1 min, stopping at −5.0 V and stepping to 0.0 V. Finally, the gauze electrode was subjected to 20 cycles at 100 mV s^{-1} between hydrogen evolution and oxygen evolution potentials (−0.26 and 1.26 V (SCE), respectively) in freshly prepared aqueous 1 M H_2SO_4 solution. This rigorous cleaning procedure was necessary to obtain reproducible results, particularly in the kinetics experiments.

Infrared spectroelectrochemistry was conducted using a Digilab FTS60V vacuum optical bench under PC control with Win-IR software. Spectra were recorded from 64 scans at 4 cm^{-1} resolution. The infrared reflection−absorption spectroelectrochemical cell contained a 9 mm diameter platinum disc working electrode, platinum wire auxiliary electrode, and SCE reference electrode. The planar platinum disc electrode was placed at 10 mm from the planar horizontal surface of a 60° beveled CaF_2 prism which provided the interface between the cell under ambient pressure and the evacuated optical bench. The infrared beam entered the thin layer of solution between the electrode and the CaF_2 prism, was reflected off the working electrode, and exited via the CaF_2 prism. Absorption spectra with this optical arrangement contain information about solution species in the thin layer and species adsorbed to the electrode surface. Details of this cell, which has a similar optical design to that of Seki et al.,[22] will be published elsewhere.[23] The platinum disc working electrode was initially polished with 0.1 μm diamond paste and then with 0.015 μm alumina powder to a mirror finish and finally sonicated in distilled water. The electrode was then given the same treatment as described above for the OTTLE cell gauze electrode. A rotatable wire grid polarizer (Cambridge Physical Sciences, IGP 228) was used to record polarized spectra.

Potential difference or SNIFTIRS spectra[24,25] were generally recorded. A base potential was chosen to obtain a background spectrum, and the electrode was held at this initial potential for 4 min. Spectra at all other potentials were presented as absorbances with respect to the background. Positive absorbance bands correspond to species produced by the potential difference while negative bands are due to the corresponding loss of reactants.

Results

Cyclic Voltammetry. Figure 1 shows first cycle cyclic voltammograms between −0.3 and 1.3 V at 100 mV s^{-1} of 10^{-3} M solutions of (a) BQH_2 and of (b) $TBQH_2$ in dichloromethane solutions. BQH_2 shows an irreversible oxidation peak at 1.10 V and a broad reduction peak at 0.41 V. $TBQH_2$ has a corresponding oxidation at 1.00 V and a reduction at 0.25 V. These oxidations are known to yield the corresponding quinones and protons, e.g., $QH_2 \rightarrow Q + 2H^+ + 2e^-$. No significant quinone production from oxidation is therefore expected at potentials less than 0.6 V. However, quinones produced by oxidation will be reduced to their radical anions at sufficiently negative potentials. In dichloromethane solution significant reduction of BQ occurs below −0.3 V and of TBQ below −0.55 V.

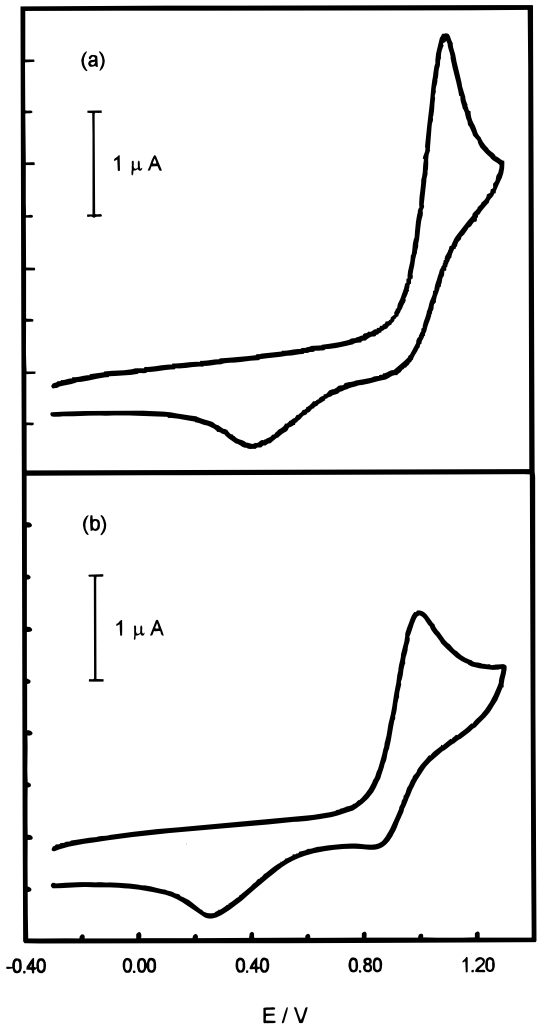

Figure 1. Cyclic voltammograms at 100 mV s^{-1} of 1×10^{-3} M solutions of (a) BQH_2 and (b) $TBQH_2$ in dichloromethane containing 0.1 M TBAP.

UV Spectroelectrochemistry. Figure 2 shows time-dependent UV absorption difference spectra of 10^{-3} M solutions of (a) BQH_2 and (b) $TBQH_2$ in the OTTLE cell containing the Pt gauze electrode under potential control. The BQH_2 data were obtained at −0.2 V while the $TBQH_2$ data were obtained at −0.4 V. Spectra were recorded repetitively at 8 nm s^{-1} with a 35.4 s cycle time. The difference spectra were obtained by subtracting the initial spectrum from each of the subsequently obtained spectra. The initial spectrum was obtained during the first scan at open-circuit potential. Spectral change was insignificant during this time under such conditions.

The difference spectra for the BQH_2 system in Figure 2a show the growth of an absorption at 245 nm and a loss of a weaker absorption at 293 nm with an isosbestic point at 267 nm. Absorption spectra of solutions of the pure compounds show that the 293 nm absorption is due to BQH_2 and the 245 nm band is from BQ. The existence of an isosbestic point confirms that BQH_2 is directly converted to BQ under these conditions. Figure 2b shows the difference spectra for the $TBQH_2$ system with the growth of an absorption at 257 nm, a loss of an absorption at 291 nm, and an isosbestic point at 275 nm. Absorption spectra of solutions of the pure compounds show

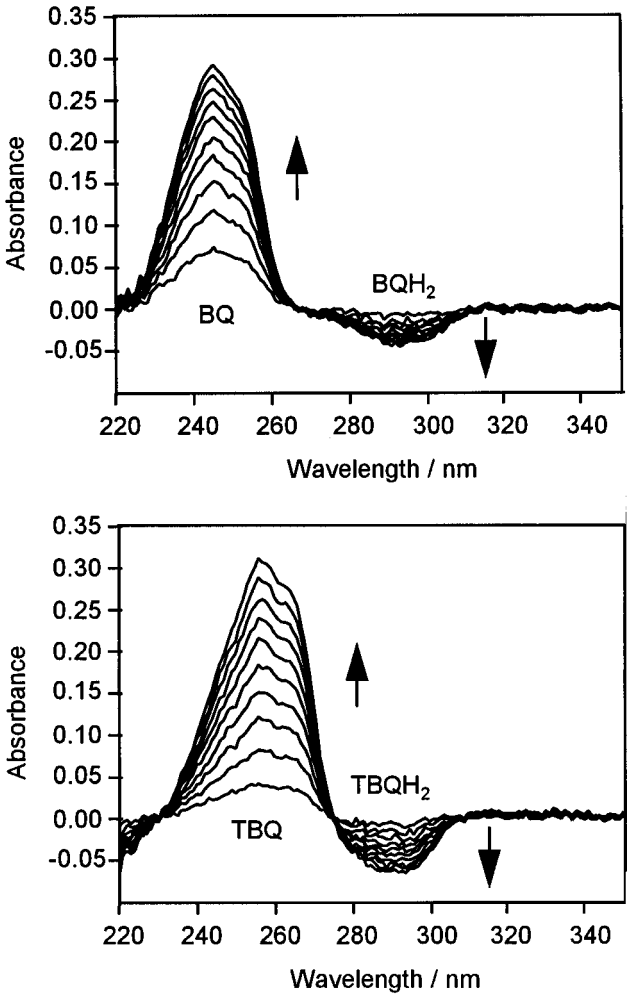

Figure 2. (a, top) UV absorption difference spectra at −0.2 V from the platinum gauze OTTLE cell of 1×10^{-3} M BQH_2 in dichloromethane containing 0.2 M TBAP. Spectra were taken at 35.4 s intervals. (b, bottom) UV absorption difference spectra at −0.4 V from the platinum gauze OTTLE cell of 1×10^{-3} M $TBQH_2$ in dichloromethane containing 0.2 M TBAP. Spectra were taken at 35.4 s intervals.

that the 291 and 257 nm bands are due to $TBQH_2$ and TBQ, respectively. The isosbestic point indicates a direct conversion from $TBQH_2$ to TBQ. Thus, both quinols undergo heterogeneous decomposition to their corresponding quinones over platinum in dichloromethane.

Initial decomposition rates were measured at fixed potentials in the potential ranges where the quinones and quinols were electroinactive. This was done by monitoring the time dependence of the absorbances at 245 nm for BQ and at 257 nm for TBQ. Figure 3 shows the decomposition rates as a function of potential for BQH_2 and $TBQH_2$. The rates were obtained using the molar absorption coefficients of BQ at 245 nm and TBQ at 257 nm of 2.19×10^6 and 1.93×10^6 M^{-1} m^{-1}, respectively.

IR Spectroelectrochemistry. The infrared spectra in Figure 4 were obtained with the IR spectroelectrochemical cell containing a 10^{-3} M BQH_2 solution without electrolyte. The spectra were solvent corrected and show the time dependence of the decomposition over about 4 min. There are increasing peak absorptions at 1672, 1658, and 1606 cm^{-1} and decreasing absorptions at 1513 cm^{-1}. Solution spectra show that the 1672 and 1658 cm^{-1} bands arise from BQ, and the 1513 cm^{-1} band is due to BQH_2. The 1606 cm^{-1} absorption arises from water, and additional bands at 3684 and 3599 cm^{-1} can verify this assignment (see Figures 4S(a) and 4S(b) of the Supporting Information).

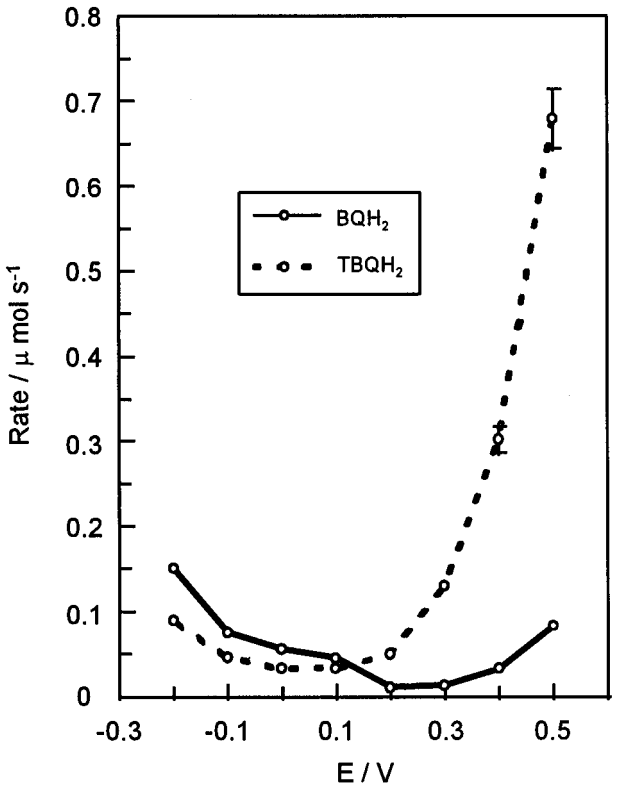

Figure 3. Potential dependence of initial decomposition rates at 25 °C of 1×10^{-3} M solutions of BQH_2 (—) and of $TBQH_2$ (- - -) in dichloromethane containing 0.2 M TBAP. Reproducibility of rates is within about 10% and is represented by error bars where this is significant in the figure.

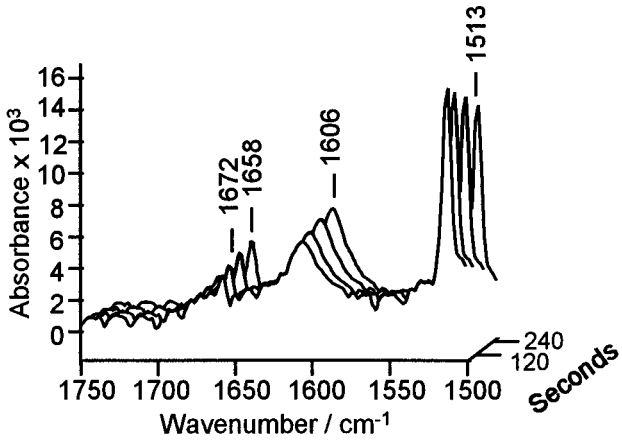

Figure 4. Time-dependent infrared spectra of a 1×10^{-3} M BQH_2 dichloromethane solution in the infrared spectroelectrochemical cell with platinum disc electrode.

The spectra obtained from a 10^{-3} M BQH_2 solution containing 0.1 M TBAP, under potential control in the IR spectroelectrochemical cell, are shown in Figure 5. Spectra were then recorded with respect to the −0.1 V background spectrum at 1 min intervals after 0.1 V steps to more positive potentials. The initial spectrum shows a loss of BQH_2 and gains of BQ and of water absorptions as well as an additional weak positive band at 1713 cm^{-1}. At more positive potentials, e.g., 0.2 V, there is a loss of BQ solution signal while the water band and the BQH_2 band (partially obscured) continue to increase and decrease respectively. Over the same range of potentials the 1713 cm^{-1} band increases steadily and further increases at potentials up to 1.2 V where BQH_2 oxidation has occurred. Also from 0.7 V, a positive band at 2340 cm^{-1} increases. This is due to CO_2

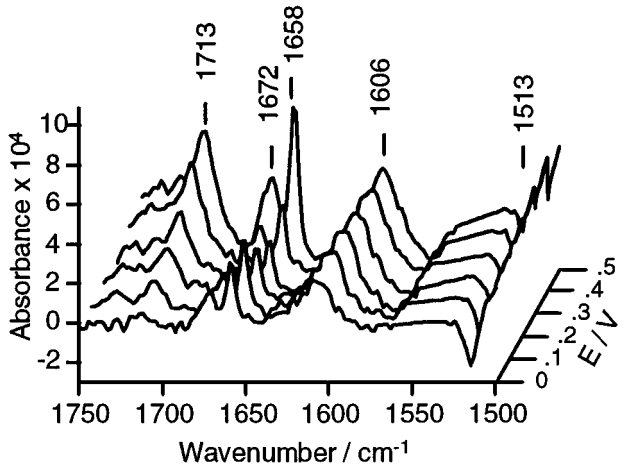

Figure 5. Potential difference infrared spectra, from the infrared spectroelectrochemical cell with platinum disc electrode, of a 1×10^{-3} M BQH_2 dichloromethane solution containing 0.1 M TBAP. Base potential −0.1 V (SCE).

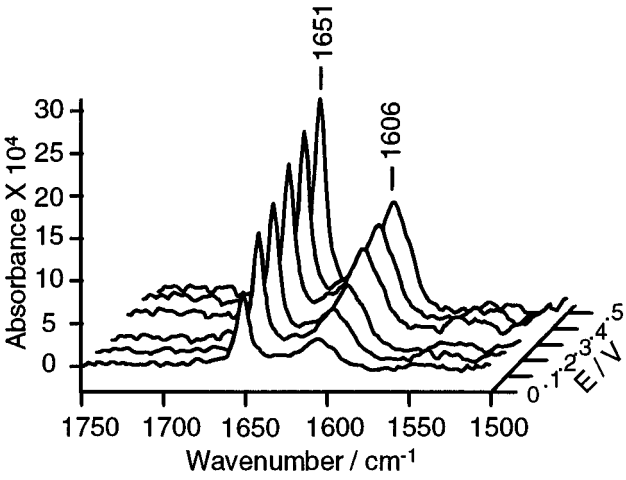

Figure 6. Potential difference infrared spectra, from the infrared spectroelectrochemical cell with platinum disc electrode, of a 1×10^{-3} M $TBQH_2$ dichloromethane solution containing 0.1 M TBAP. Base potential −0.1 V (SCE).

arising from some irreversible electrochemical oxidation of adsorbed BQ and /or BQH_2.[1,13]

The results of the corresponding infrared spectroelectrochemical experiment with 10^{-3} M $TBQH_2$ are shown in Figure 6. Positive potential steps from a base potential of −0.1 V showed growth of a TBQ peak at 1651 cm^{-1} and a water peak at 1606 cm^{-1}. There is also a weak negative band at 1520 cm^{-1}, partially hidden by the view chosen, due to loss of $TBQH_2$. There is no absorption at higher wavenumbers corresponding to that observed in the BQH_2 experiments.

The association of the 1713 cm^{-1} band with BQ was made in the following experiment. A 2×10^{-3} M solution of BQ containing 0.1 M TBAP in dichloromethane was placed in the spectroelectrochemical cell with the Pt working electrode held at 0.9 V for 5 min. A potential of 0.2 V was then used as background for the subsequent spectra taken at 0.1 V steps to more negative potentials and at 1 min intervals. Figure 7 shows the resultant spectra. The absorptions of BQ in solution at 1658 and 1672 cm^{-1} begin to decrease at −0.4 V as reduction of BQ to $BQ^{\bullet-}$ commences. From −0.5 V there is an additional weak absorption loss at 1713 cm^{-1} which follows the trend in the solution BQ signal. There is no 1713 cm^{-1} band in infrared spectra of BQ solutions.

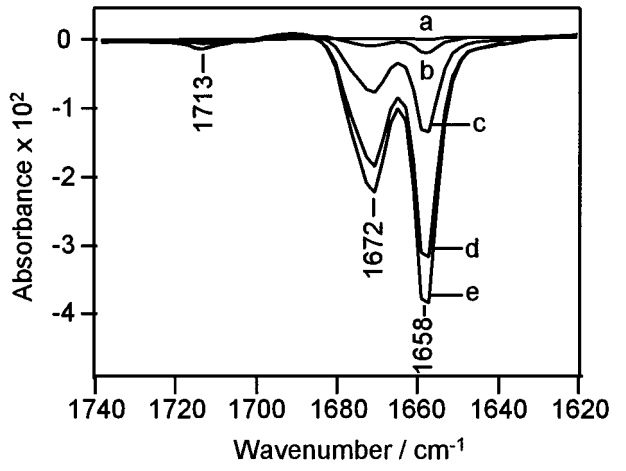

Figure 7. Potential difference infrared spectra, from the infrared spectroelectrochemical cell with platinum disc electrode, of a 2×10^{-3} M BQ dichloromethane solution containing 0.1 M TBAP. (a) −0.3 V, (b) −0.4 V, (c) −0.5 V, (d) −0.6 V, (e) −0.7 V (SCE). Base potential 0.2 V (SCE).

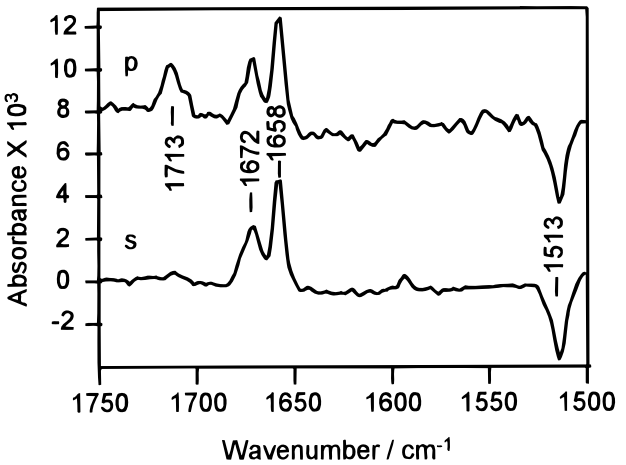

Figure 8. Polarized potential difference infrared spectra, from the infrared spectroelectrochemical cell with platinum disc electrode at $E = 0.8$ V (SCE), of a 1×10^{-3} M BQH_2 dichloromethane solution containing 0.1 M TBAP. Base potential −0.1 V (SCE). The absorbance scale is for the s-polarized spectrum. The p-polarized spectrum has been rescaled for comparison.

Polarised infrared radiation may be used to identify adsorbates and to determine surface orientation.[25] Figure 8 shows the p- and s-polarized infrared spectra from the spectroelectrochemical cell of a 10^{-3} M BQH_2, 0.1 M TBAP solution in dichloromethane at 0.8 V with respect to a −0.1 V base potential. Comparison of the intensity of the 1713 cm^{-1} band with those of solution BQ in Figure 8 shows that the 1713 cm^{-1} peak is strong in the p-polarized spectrum but insignificant in the s-polarized spectrum.

Discussion

The results of the time-dependent and controlled potential infrared spectroscopy experiments as shown in Figures 4 and 5 indicate that BQ and water are products of BQH_2 decomposition. The quinone and water are also products of the decomposition of $TBQH_2$ at potentials less than required for $TBQH_2$ oxidation. Previously, studies of BQH_2 adsorption at platinum electrodes in acidic aqueous solutions have suggested that molecular hydrogen is a product of dehydrogenative decomposition.[11] No evidence has been presented in support of this hypothesis. The present results from dichloromethane solutions point to surface

oxides as the source of oxygen in the formation of water during the decomposition.

There is a distinct potential dependence of the heterogeneous decomposition rates of the quinols as shown in Figure 3. In general, the decomposition rates of both quinols show a minimum between 0.0 and 0.2 V. There are significant increases in decomposition rate to more negative potentials. However, there are also decomposition rate increases to more positive potentials with those of $TBQH_2$ being much more pronounced.

It appears that, as soon as hydroquinones reach the surface, they dehydrogenate immediately. In the potential range between 0 and 0.2 V, which is close to the double-layer region for aqueous systems, the concentration of the adsorbed hydrogens may be high. Hydrogen atoms can adsorb strongly to a Pt surface and perturb the adsorption of quinols in aqueous systems.[4] This hydrogen adsorption hinders quinol adsorption and decomposition. Adsorbed hydrogen atoms can also react with any adsorbed oxygen atoms to produce some water.

As the potential increases beyond 0.1 V, the oxidation of adsorbed hydrogen atoms to protons begins. This phenomenon causes a decrease in the surface concentration of hydrogen and an increase in the rate of quinol decomposition. Of the quinol decomposition products, BQ is able to adsorb endwise (η^1) via the carbonyl oxygen atom. However, TBQ is unlikely to adsorb in this manner due to the steric hindrance of the *tert*-butyl groups. It is significant that no extra band at about 1713 cm^{-1} due to adsorbed TBQ is observed. It is therefore likely that the relatively low apparent decomposition rate of BQH_2 is due to competition for adsorption between BQ and BQH_2, resulting in a lower availability of surface sites for BQH_2 decomposition. The lack of evidence for TBQ adsorption suggests that $TBQH_2$ decomposition sites have a higher availability, resulting in a higher decomposition rate under these conditions.

At potentials less than 0.1 V, evolution of molecular hydrogen is expected. This process would facilitate decomposition of quinols on platinum. In this potential range, $TBQH_2$ has a lower decomposition rate. No extra band is observed at 1713 cm^{-1} due to adsorbed BQ, nor is there any evidence for adsorption of TBQ. Thus, the lower $TBQH_2$ decomposition rate is probably due to the steric hindrance, from the bulky *tert*-butyl groups, preventing the close approach of the $TBQH_2$ molecule to the platinum surface.

The new absorption at 1713 cm^{-1} in the infrared spectroelectrochemical results given in Figures 5, 7, and 8 has been shown to be due to an adsorbed BQ species. The Figure 8 data indicate that there is a BQ absorption arising from a group that has a dipole moment change with a component of vibration normal to the electrode surface. This must be the C═O group of BQ adsorbed endwise on platinum.

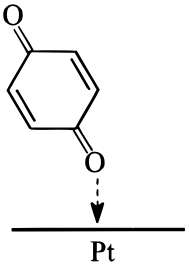

Conclusion

BQH_2 and $TBQH_2$ undergo heterogeneous decomposition at a platinum surface in dichloromethane solution to form BQ and TBQ, respectively. These decomposition processes are potential dependent with minimum rates corresponding to conditions under which adsorbed hydrogen atoms, also products of the decompositions, are expected to be present. The potential dependence of the decomposition rates reflects the competition for surface sites between the quinols and adsorbed hydrogen atoms. At positive potentials the decomposition rate of BQH_2 is lower than that of $TBQH_2$ due to BQ adsorption. Previous studies of quinol adsorption and decomposition on platinum electrodes in aqueous systems have pointed to decomposition via a η^6 (flat) orientation leading to the corresponding η^6-adsorbed quinone. However, this study indicates that, with dichloromethane solutions at more positive potentials, endwise adsorption of BQ also occurs. This is not surprising considering the low dielectric constant of the solvent and the polarity of the quinone oxygens. The corresponding adsorption of TBQ was not observed and is sterically prohibited.

Acknowledgment. A.B. acknowledges a scholarship from the Ministry of Culture and Higher Education of Iran. This work was supported by the Research Committee and the Division of Sciences of the University of Otago.

Supporting Information Available: Infrared spectra in the 4000−1460 cm^{-1} range of (a) a 1% solution of water in dichloromethane, from a 50 mm film in a transmission cell with solvent absorptions subtracted, and (b) Figure 4 at 240 s with the wavenumber range to 4000 cm^{-1} included (2 pages). Ordering information is given on any current masthead page.

References and Notes

(1) Hubbard, A. T. *Chem. Rev.* **1988**, *88*, 633.
(2) Lane, R. F.; Hubbard, A. T. *J. Phys. Chem.* **1973**, *77*, 1401.
(3) Chia V. K. F.; Stickney, J. L.; Soriaga, M. P.; Rosasco, S. D.; Salaita, G. N.; Hubbard, A. T.; Benziger, J. B.; Pang, K. W. P. *J Electroanal. Chem.* **1984**, *163*, 407.
(4) Chia, V. K. F.; Soriaga, M. P.; Hubbard, A. T. *J. Electroanal. Chem.* **1984**, *167*, 97.
(5) White, J. H.; Soriaga, M. P.; Hubbard, A. T. *J. Electroanal. Chem.* **1985**, *185*, 331.
(6) Krauskopf, E. K.; Wieckowski, A. *J. Electroanal. Chem.* **1990**, *296*, 159.
(7) Michelhaugh, S. L.; Carrasquillo, A.; Soriaga, M. P. *J. Electroanal. Chem.* **1991**, *319*, 387.
(8) Soriaga, M. P. ; Wilson, P. H.; Hubbard, A. T.; Benton, C. S. *J. Electroanal. Chem.* **1982**, *142*, 317.
(9) Soriaga, M. P.; Hubbard, A. T. *J. Am. Chem. Soc.* **1982**, *104*, 2735.
(10) Soriaga, M. P.; Hubbard, A. T. *J. Am. Chem. Soc.* **1982**, *104*, 3937.
(11) Chia, V. K. F.; Soriaga, M. P.; Hubbard, A. T. *J. Phys. Chem.* **1987**, *91*, 78.
(12) Pang, K. P.; Benziger, J. B.; Soriaga, M. P., Hubbard, A. T. *J. Phys. Chem.* **1984**, *88*, 4583.
(13) Soriaga, M. P.; White, J. H.; Song, D.; Chia, V. K. F. ; Arrhenius, P. O.; Hubbard, A. T. *Inorg. Chem.* **1985**, *24*, 73.
(14) Song, D.; Soriaga, M. P.; Vieira, K. L.; Zapien, D. C.; Hubbard, A. T. *J. Phys. Chem.* **1985**, *89*, 3999.
(15) Song, D.; Soriaga, M. P.; Hubbard, A. T *J. Electroanal. Chem.* **1986**, *201*, 153.
(16) Song, D.; Soriaga, M. P.; Hubbard, A. T. *J. Electrochem. Soc.* **1987**, *134*, 874.
(17) Hubbard, A. T. *J. Vac. Sci. Technol.* **1980**, *17*, 49.
(18) Clark, B. R.; Evans, D. *J. Electroanal. Chem.* **1976**, *69*, 181.
(19) House, H. O.; Feng, E.; Peet, N. P. *J. Org. Chem.* **1971**, *36*, 2371.
(20) Fry, A. J.; Britton, W. E. In *Laboratory Techniques in Electroanalytical Chemistry*; Kissinger, P. T.; Heineman, W. R., Eds.; Marcel Dekker: New York, 1984; p 367.
(21) Gamage, R. S. K. A.; McQuillan, A. J.; Peake, B. M. *J. Chem. Soc., Faraday Trans.* **1991**, *87*, 3653.
(22) Seki, H.; Kunimatsu, K.; Golden, W. G. *Appl. Spectrosc.* **1985**, *39*, 437.
(23) Brooksby, P. A.; Love, J. G.; McQuillan, A. J. To be published.
(24) Ashley, K.; Pons, S. *Chem. Rev.* **1988**, *88*, 673.
(25) Iwasita, T.; Nart, F. C. In *Advances in Electrochemical Science and Engineering*; Gerischer, H.; Tobias, W., Eds.; VCH: Weinheim, 1995; Vol. 4, p 126.